GeoScienceWorld
Lithosphere
Volume 2022, Article ID 7161484, 15 pages
https://doi.org/10.2113/2022/7161484

Lithosphere

Research Article

Hot or Fertile Origin for Continental Break-Up Flood Basalts: Insights from Olivine Systematics

Jackson Stone Borchardt and Cin-Ty Lee

Department of Earth, Environmental and Planetary Sciences, Rice University, MS-126, 6100 Main Street, Houston, TX 77005, USA

Correspondence should be addressed to Jackson Stone Borchardt; jsb13@rice.edu

Received 26 May 2022; Revised 17 October 2022; Accepted 1 November 2022; Published 28 November 2022

Academic Editor: Zheng Zhou

The break-up of supercontinents is often temporally and spatially associated with large outpourings of basaltic magmas in the form of large igneous provinces (LIPs) and seaward dipping reflectors (SDRs). A widespread view is that the upwelling of hot mantle plumes drives both continental break-up and generation of associated LIPs. This is supported by petrologic estimates of the temperature from olivine-melt thermometers applied to basaltic magmas. These thermometers must be applied to a primary mantle-derived magma, requiring the selection of an appropriate primitive magma and an assumption of how much olivine is to be back-added to correct for fractional crystallization. We evaluated the effects of these assumptions on formation temperatures by compiling and analyzing a database of North Atlantic igneous province (NAIP) and Central Atlantic magmatic province (CAMP) lavas and olivines. Ni and FeO_T systematics suggest that many picrite magmas have undergone olivine addition and are not true liquids, requiring careful selection of primitive magmas. The maximum amount of back-added olivine was determined by constraining mantle peridotite melt fractions for a range of possible mantle potential temperatures and continental lithosphere thicknesses. Using an empirical relationship between melting degree and forsterite (Fo) content, we show that the possible maximum olivine forsterite content in equilibrium with NAIP magmas is 90.9, which is lower than the maximum olivine forsterite content observed in the NAIP olivine population. We infer primary magmas that lead to mantle potential temperatures of 1420°C for the NAIP and 1330°C for CAMP. Using a similar approach for consistency, we estimate a mantle potential temperature of 1350°C for mid-ocean ridge basalts (MORB). Our results suggest that LIPs associated with continental break-up are not significantly hotter than MORB, which suggests that continental break-up may not be driven by deep-seated thermal plumes. Instead, we suggest that such voluminous magmatism might be related to preferential melting of fertile components within the lithosphere triggered by far-field extensional stresses.

1. Introduction

Over geologic time, the distribution of Earth's continents has fluctuated between amalgamated supercontinent states and dispersed states, such as today [1]. These changes in continental configuration are fundamentally related to deep Earth processes [1, 2]. The distribution of continents may influence ocean and atmospheric circulation, depositional environments, and the nature of continental erosion and weathering. Because of interactions between the deep Earth and the surface, supercontinent cycles may be important for controlling long-term climate and environmental conditions. For example, supercontinent dispersal has been suggested as a possible control on snowball Earth glaciations [3, 4], oxygenation events [5], global benthic microbial activity [6], and the evolution of life [7] in the Neoproterozoic era.

Despite the importance of supercontinent cycles, the processes that initiate supercontinent break-up are still debated [8–12]. Any hypothesized mechanism for continental break-up must explain the temporal association of break up with the appearance of large igneous provinces (LIPs), manifested as large outpourings of flood basalts and thick dipping layers of basalt on continental margins (known as seaward dipping reflectors, SDRs) [8]. The most popular continental break-up theory, the mantle plume hypothesis, invokes a deep-seated thermal anomaly in the mantle that rises as a plume from a hot thermal boundary layer at the

base of the mantle. Because of its thermal buoyancy, the plume is thought to initiate continental break-up and simultaneously give rise to extensive basaltic volcanism [12–14]. Consistent with a thermal plume hypothesis, petrological studies of various continental flood basalts have estimated flood basalt mantle source temperatures to be 160 to 230°C higher than ambient mantle [15–17].

All petrologic estimates of mantle source temperatures, however, are based on olivine-liquid thermometry, which relies on the temperature-dependent olivine/melt partitioning of Fe and Mg. An important property of Fe and Mg systematics in olivine is that although the individual Fe and Mg partition coefficients are temperature sensitive, the temperature sensitivities of Fe and Mg are similar, resulting in a relatively constant Fe-Mg exchange coefficient [18]. This property allows the temperature of a magma to be estimated from its MgO content alone, provided that the magma is in equilibrium with olivine. However, to estimate the temperature of the mantle source, the primary mantle-derived magma must be known. Because most magmas, even primitive ones, have already differentiated by the time they reach the surface, the primary magma composition must be inferred by back-adding olivine into the melt to reverse the effects of crystal fractionation [9, 15, 18, 19]. In this text, we follow the nomenclature of Herzberg et al. [19] where a primitive magma is a magma that has only undergone olivine fractionation, and a primary magma is a primitive magma that has been corrected back to its original forsterite content and presumably in equilibrium with its mantle source.

Application of olivine-liquid equilibrium thermometry depends on two critical assumptions: the forsterite (Fo) content of olivine in the residual mantle source and the total iron content (expressed as FeO_T) of the primitive magma to be corrected for fractionation. These two quantities are important because they dictate how much olivine must be added until equilibrium with an assumed residual mantle is attained, and it is the amount of back-added olivine that controls the primary MgO content, which in turn controls the temperature of the hypothetical primary mantle-derived magma. As shown in Figure 1, adding more olivine or starting with a primitive magma with high FeO_T content will result in a calculated primary magma with high MgO and high temperatures, while correcting to a lower Fo content or starting at a lower FeO_T will result in lower temperatures [10, 20]. Herzberg and O'Hara [21] attempted to circumvent this problem by matching the back-calculated primary magma with modeled primary melts produced by peridotite melting. A more recent aluminum in olivine thermometer developed by Coogan et al. [22] and Wan et al. [23] allows temperature to be determined from olivine instead of the melt, which may reduce uncertainties in estimating primary magma compositions because early-crystallized grains are often preserved in olivine populations. However, this method is not without challenges as equilibrium olivine composition still must be known or back-calculated, compositions of coexisting spinel must be known, and Al contents in olivine may be vulnerable to kinetic effects due to Al's slow diffusivity [24–26].

Here, we revisit the problem of estimating primary magma temperatures by examining olivine and whole-rock compositions from the North Atlantic igneous province (NAIP) and the Central Atlantic magmatic province (CAMP), both of which are associated with continental break-up in the Paleogene and at the beginning of the Jurassic. Estimating primary magma temperatures for mid-ocean ridge basalts (MORBs) is particularly challenging because most MORBs are far too evolved to perform an olivine correction. Siqueiros on the East Pacific Rise is one of the few ridge sites that host primitive MORBs on olivine-control lines [27]. Below, we reevaluate methods of estimating primary magma compositions and show that primary magma temperatures of some LIPs may have been overestimated. The tectonic and magmatic implications of a weakened thermal anomaly are discussed.

1.1. Geologic Background and Previous Work. The NAIP formed continental flood basalts and intrusive and extensive seaward dipping reflectors (SDRs) as Greenland, Europe, and Canada dispersed [28]. The bulk of the magmatism occurred from 62 to 55 Ma, with smaller eruptions continuing until 15 Ma [29]. The North Atlantic was fully opened ~55 Ma during the early Eocene but was preceded by sporadic and limited extension beginning at 400 Ma [30–32].

The Central Atlantic magmatic province (CAMP) formed 201 Ma as Africa, South America, and North America separated, with magmatism postdating the initiation of extension by ~25 My [33–35]. Most CAMP flows have since been eroded, but sills, dikes, minor flows, and associated SDRs remain, with outcrops appearing in eastern USA, Morocco, Spain, and Brazil [34]. Previous work suggested that CAMP was formed from a plume [36], but no thermal anomaly has yet been inferred petrologically [15].

Siqueiros, near the East Pacific Rise, was chosen because these are the most primitive MORB samples and therefore on an olivine control line [27]. Because of the primitive nature of this MORB suite, Putirka [10] used Siqueiros as a baseline to compare to LIPs and SDRs.

2. Methods

For each province, all olivine mineral data and whole-rock data with a SiO_2 less than 52% were downloaded from the EarthChem online database and then further supplemented with a literature review (http://earthchem.org/portal). Full recognition of all sources of data is not possible here, but the compiled data and complete reference list are included in supplementary file 1. The compilation is especially reliant on the following works: for the NAIP [37–42], for the CAMP [43–46], and for Siqueiros [27, 47–49].

Duplicates and any samples that did not have complete major element information were excluded. Whole-rock compositions were then normalized to a 100% volatile-free basis. To evaluate overall systematics, whole-rock samples were binned over intervals of 2 Mg# units [molar $Mg/(Mg + Fe \times 100)$]. In the bulk-rock samples, we convert any reported Fe_2O_3 to FeO and report the new value as FeO_T. For each Mg# bin, the mean of each major and trace element

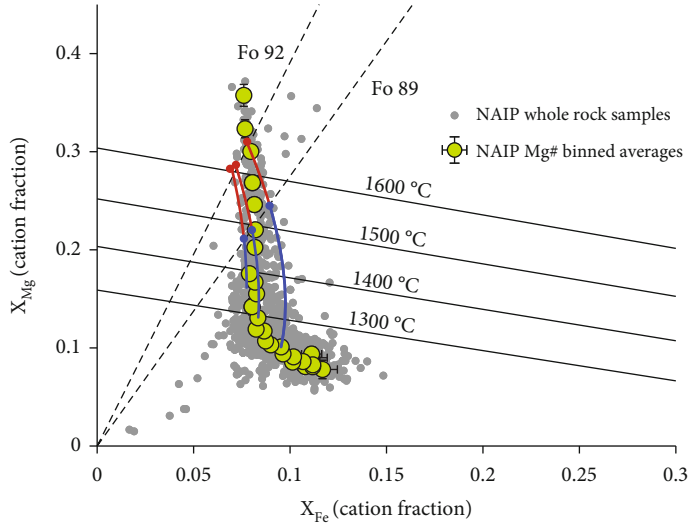

FIGURE 1: A modified Roeder and Emslie plot of X_{Mg} vs. X_{Fe} from Putirka [10]) for the investigated NAIP whole-rock samples, plotted both as individual data and as Mg#-binned averages (see text). Isotherms are calculated from Putirka's [10] compositional independent A and B models. The red and blue lines show the liquid composition as equilibrium olivine is back-added at a fixed $K_D\,(Fe-Mg)^{Ol-liq}$ of 0.34. Blue line is the melt's evolution until it is in equilibrium with Fo 89. Red line is in equilibrium with Fo 92. Dashed lines are olivine compositions. Small changes in the Fo content of the source have large implications for the temperature of magma.

concentration and isotope ratio was calculated along with the standard error. For ratios of elements, individual ratios were first calculated and then binned by Mg# before taking the mean value of the ratios.

3. Results

Figure 2 tracks how Ni, Fe, and Mg evolve for whole-rock and olivine samples from the investigated LIPs and MORB. The Mg# or the MgO content of the magma is commonly used as a differentiation index. The binned average Mg# of the whole-rock samples evolves from 82 to 29 for NAIP, 75 to 24 for CAMP, and 74 to 26 for MORB. Over the same interval, MgO contents evolve from 28 to 6 for NAIP, 15 to 3 for CAMP, and from 18 to 3 for MORB. Overall, these provinces show tholeiitic-type differentiation, with whole-rock FeO_T increasing with differentiation (decreasing Mg# and MgO). However, there are differences in initial FeO_T, defined as the FeO_T of the highest Mg#-binned average: initial FeO_T is 10.6 wt.% for NAIP, 8.3 wt.% for CAMP, and 8.4 wt.% for MORB. Ni, a compatible element in olivine, decreases rapidly with differentiation, but the magnitudes of the decrease differ in detail. The Ni content of the highest Mg# whole-rock samples for each province is 1280 ppm for the NAIP, 288 ppm for CAMP, and 320 for MORB. Mg#-binned average Ni for the NAIP decreases monotonically.

In Figure 3, we examine the weight ratios of Fe/Mn, Zn/Fe, and CaO/Al_2O_3 versus Mg# from the binned whole-rock data. These trace and major elements are sensitive to different lithologies in the mantle source. Fe/Mn, Zn/Fe, and CaO/Al_2O_3 ratios are minimally affected by olivine crystallization but are influenced by the presence of pyroxene in the source [50, 51]. Melting of a pyroxenite source will produce primitive melts with elevated ratios of Fe/Mn, Zn/Fe, and CaO/Al_2O_3. At low Mg#s, when pyroxene, magnetite, or plagioclase saturates in the magma, these ratios evolve and reflect later stage magma differentiation processes, which are not of interest here. We focus here on only the primitive magmas (Mg# 70-72). For primitive magmas, Fe/Mn ratios are 60 for the NAIP, 57 for CAMP, and 71 for MORB. Primitive Zn/Fe ratios are indistinguishable: 0.99×10^{-3} for NAIP, 1.0×10^{-3} for CAMP, and 0.99×10^{-3} for MORB. The CaO/Al_2O_3 ratio is 0.82 for the NAIP, 0.74 for CAMP, and 0.68 for MORB. All of these values are consistent with peridotite melting (as defined by experiments from Le Roux et al. [50]) or similar to MORB, suggesting that the majority of the source for CAMP and NAIP is peridotite.

4. Discussion

The main challenge in calculating primary magma temperatures based on olivine-liquid equilibria is that the primary magma is never sampled. All magmas undergo some level of fractional crystallization before erupting. Thus, the largest uncertainties, ironically, are not in the accuracy of olivine-liquid thermometers but in identifying the primitive magma and correcting for fractionation. The fractionation correction requires determining the amount of olivine that must be added back to reverse the effects of crystallization. Here, we first evaluate what constitutes a primitive magma in each investigated province. We then show that the Fo content of an olivine is related to the degree of melting of a peridotite mantle source. Then, using compiled olivine compositions for each province, we calculate hypothetical maximum and minimum temperatures for the primitive melts of each province. We use the range of hypothetical temperatures, the relationship between Fo and melting degree, and a peridotite-melting model to constrain the highest possible Fo content for a primary magma. Using this new Fo content,

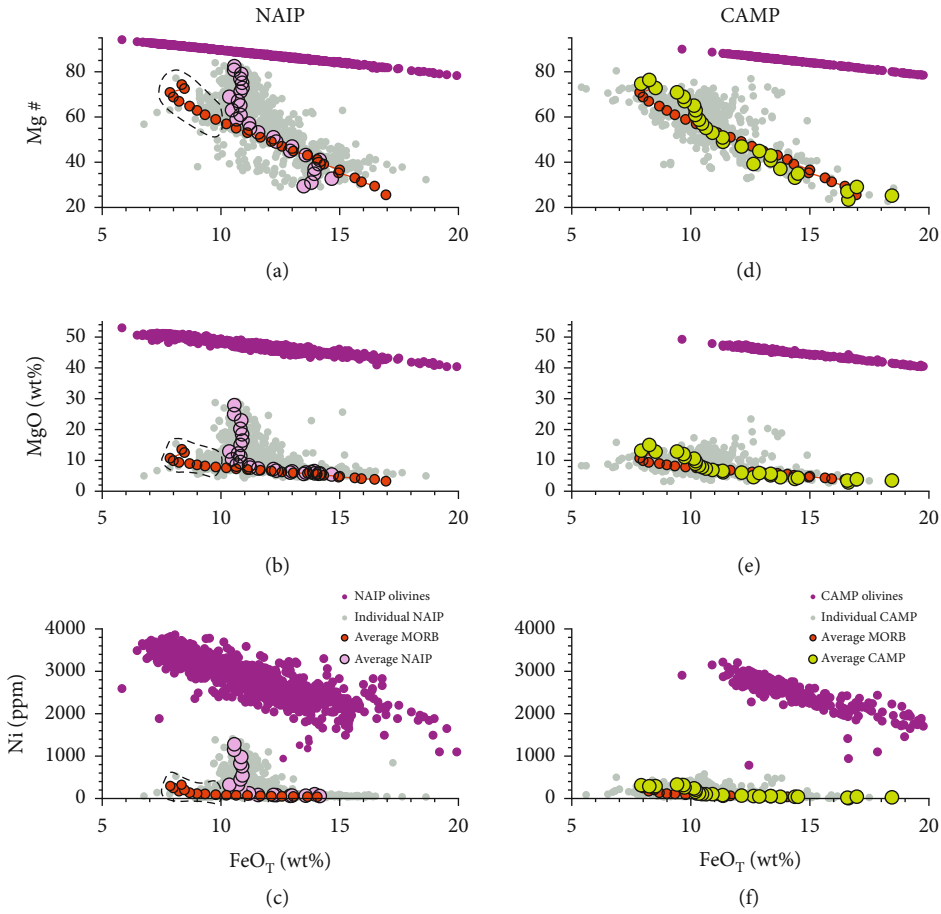

Figure 2: LIPs plotted against MORB, with individual basalt samples in grey, olivines in purple, NAIP average basalts in pink, CAMP average basalts in green, and MORB averages in red. Note in the NAIP the low Fe low Ni samples, highlighted with the black dashed line, that follow the average MORB trend. The main trend of NAIP data is drawn towards the olivine cloud, arguing for mixing process.

we calculate new mean mantle potential temperatures for each province.

4.1. Distinguishing Primitive Magmas from those with Accumulated Olivine. A first-order control on reconstructing primary magma compositions is to identify the most primitive magma, that is, one that has undergone as little fractional crystallization as possible so that uncertainties in correcting for fractionation are minimized. In practice, this involves taking the least-evolved magma as determined by Mg# or MgO. However, care must be taken because olivine accumulation can result in a crystal-rich magma, whose bulk composition appears primitive in terms of MgO or other compatible elements but does not represent an actual melt composition because it is a mixture of melt and excess amounts of olivine. Because Fe has an olivine/melt partition coefficient of approximately 1, accumulation or fractionation of olivine does not significantly change a magma's FeO$_T$ content [18] (Figure 1). As such, excess olivine in a magma may go unnoticed when examining Fe-Mg systematics. In contrast, Ni is highly compatible in olivine so that even small amounts of olivine fractionation or accumulation yield significant changes in Ni [52, 53]. For these reasons, we use Ni-FeOT systematics to detect olivine accumulation.

In the NAIP, FeOT and Ni relationships suggest that high MgO (15-28 wt.% MgO) picrite lavas may have undergone olivine addition, and that magmas with Ni and FeO$_T$ values less than 320 ppm and 10.5 wt.%, respectively, are magmas that best represent true liquids (Figure 2(c)). The highest MgO and Mg# magmas define an array that extends toward the olivine cloud in the NAIP, a feature usually interpreted to represent olivine fractionation, where olivine segregation causes MgO, Ni, and Mg# to decline at relatively constant FeO$_T$. However, the same array can also be explained by olivine accumulation. In this context, it is noteworthy that not all primitive samples in the NAIP fall on this olivine fractionation/addition array as some samples (highlighted by black dashed line) have lower FeO$_T$, Ni, and MgO contents but otherwise have Mg#s as high as 70. Because the crystal/melt partition coefficient of FeO in olivine is close to 1, it is not possible to form these low FeO$_T$ magmas from the high FeO$_T$ magmas by fractional crystallization of olivine. Given their high Mg#s, the low FeO$_T$ and Ni contents of these magmas are clearly not the result of fractionation of pyroxene or magnetite. We interpret them as true primitive magmas, whereas the high Ni, MgO, and FeO$_T$ magmas have been modified by olivine accumulation so that their compositions do not represent true liquids.

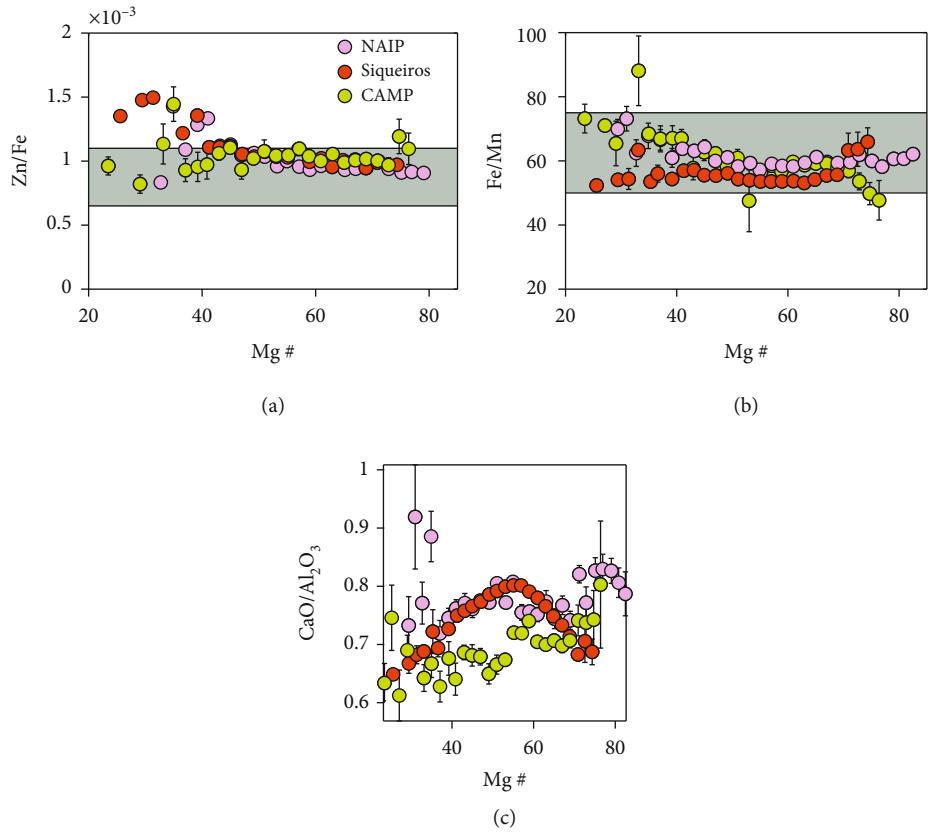

Figure 3: LIPs compared to MORB for multiple mantle heterogeneity tracers. Samples are Mg#-binned averages. Error bars represent the standard error of the mean. If no error bars are observed, it is because they are smaller than the marker size. Typical range in values for a melt from a peridotite source is in grey [50]. The LIPs show no significant difference from MORB for the tracers, suggesting a peridotite source.

High Mg# magmas in CAMP and MORB have previously been attributed to olivine addition [27, 54]. For this study, we select primitive magma compositions after excluding those samples that show olivine addition in Ni-FeO space. An important outcome of this analysis is that the FeO_T content estimated for primitive magmas must be revised to lower values and, as we have discussed above, lower initial FeO_T results in lower temperatures for calculated primary magmas.

After filtering for olivine accumulation, the most primitive magma for the NAIP is sample 176611 from [40]: Mg#~68, MgO~10.7 wt.%, and FeO_T~9.1 wt.%. For CAMP, the most primitive magma is W-243838 from [55] with a Mg# of 69, MgO of 10.4 wt.%, and FeO_T of 8.4 wt.%. Finally, for Siqueiros, sample AII1991-020-015 from [27] was taken as the most primitive magma (Mg#~69, MgO~9.9 wt.%, and FeO_T~7.9 wt.%).

4.2. Equilibrium Forsterite Effect on Primary Magma Temperature and Pressure. To accurately capture the initial formation conditions of a basaltic magma, it is necessary to correct for olivine fractionation by back-adding olivine in small increments until it is in equilibrium with its original source. The challenge is that we do not know when to stop adding olivine because the Fo content of the olivine in the mantle source is not known. Previous studies have approached this challenge in three different ways. In one approach, olivine is added until the melt reaches equilibrium with a universal Fo content, such as 89 or 90, values typically attributed to primitive mantle [20, 56]. In a second approach, olivine addition is terminated when the magma equilibrates with the maximum-observed Fo olivines [10, 57]. In the third approach, olivine addition is terminated when the magma is in equilibrium with some average (either calculated or assumed) between a primitive mantle Fo and the highest-observed Fo [24].

Here, we propose melt fraction as constrained by lithospheric thickness as one measure of an upper bound on how much olivine can be added to a fractionated magma. Melting experiments of fertile peridotite from Walter [58] show a systematic correlation between melting degree (%) and the Fo content of residual olivine, with the slope of the linear correlation ranging from 15.0-15.7% melt fraction/Fo. The slope of the correlation remains relatively insensitive to pressure in the 3-7 GPa range, which is the pressure range most relevant to the generation of basaltic magmas. Using this empirical relationship, NAIP olivines with Fo > 93 can only be attained by peridotite-melting degrees of >60%, assuming an Fo of 89.3 lherzolitic starting composition (Figure 4(a)). Are these high melt fractions realistic for an

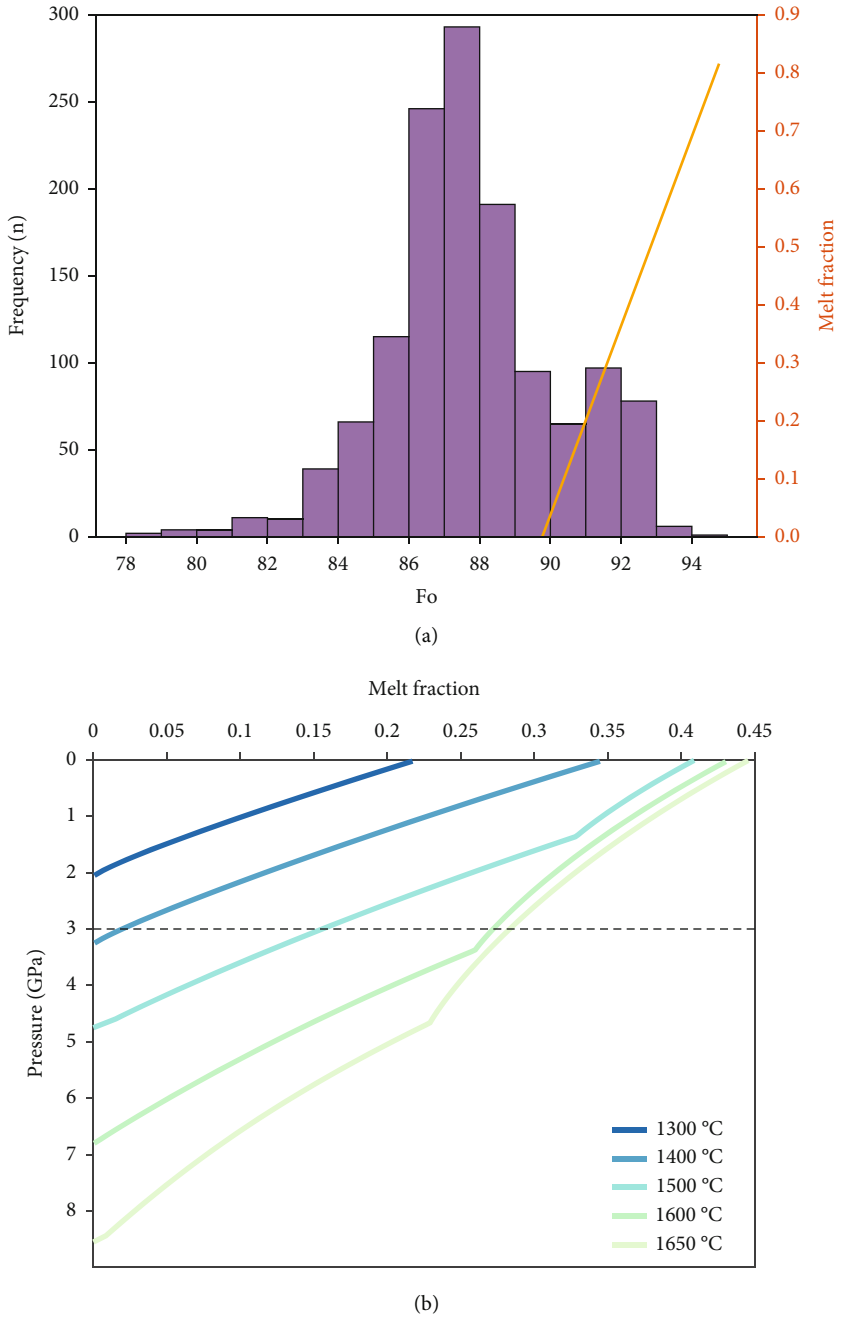

Figure 4: (a) A histogram of the Fo content of olivines from all NAIP lavas. Orange line represents the melt fraction necessary to generate olivine of a specific Fo content in residual mantle (right hand vertical axis) based on 3 kbar peridotite-melting experiments from Walter [58] (see text for discussion). The highest Fo olivine in the NAIP would require a primary mantle-derived magma that is formed by ~67% melting. (b) Calculated melt fractions for a package of adiabatically rising dry lherzolite mantle. Each line corresponds to a different solid mantle potential temperature. Melt fractions are calculated following Katz et al. [62], with an initial clinopyroxene mode of 20% assumed. Higher mantle potential temperature results in greater initial melting depths. Dashed horizontal line at 3 GPa corresponds to a representative continental lithosphere thickness at the time of LIP emplacement. This depth limits the extent to which the mantle can decompress. This limit of decompression, combined with the highest possible mantle potential temperature for the NAIP, limits the highest melt fraction possible to <30%, corresponding to a maximum Fo of 90.9, far lower than the highest Fo contents measured in NAIP olivines.

ascending mantle plume under continental lithosphere, which is invariably thicker than the lithosphere beneath mid-ocean ridges?

In order to access the variability of melt fraction in LIPs, we need a range of possible temperatures that LIPs formed at. To estimate this range, we compiled all available olivine phenocryst data for our case studies. Using the primitive lava selected by the approaches described in the previous section, we back-added olivine to match three different Fo contents assuming each increment of olivine is in

Table 1: Compositions of primary magmas. Compositional differences of primary magmas due to changes in assumptions of equilibrium Fo. The $K_D\,(Fe-Mg)^{Ol-liq}$ is changed between a fixed and evolving composition to show the effect on the final composition of the magma. See text for details.

Province	Fo	KD	SiO_2	TiO_2	Al_2O_3	FeO	MgO	CaO	Na_2O	K_2O	P_2O_5	MnO	Fe_2O_3
NAIP	89	0.32	47.7	0.8	15.7	8.3	12.2	12.4	1.5	0.2	0.1	0.1	1.0
	94.2	0.32	45.8	0.5	11.0	8.1	23.8	8.7	1.1	0.1	0.0	0.1	0.7
	91	0.32	47.1	0.7	14.3	8.4	15.5	11.3	1.4	0.2	0.1	0.1	0.9
	90.9	0.32	47.1	0.7	14.3	8.4	15.3	11.3	1.4	0.2	0.1	0.1	0.9
	89.9	0.32	47.4	0.7	15.1	8.4	13.6	11.9	1.5	0.2	0.1	0.1	0.9
	89	Evolve	47.7	0.8	15.6	8.3	12.4	12.3	1.5	0.2	0.1	0.1	1.0
	94.2	Evolve	45.4	0.5	10.1	8.1	26.0	8.0	1.0	0.1	0.0	0.1	0.6
	91	Evolve	46.9	0.7	13.9	8.5	16.4	11.0	1.4	0.2	0.1	0.1	0.9
	90.9	Evolve	47.0	0.7	14.0	8.5	16.1	11.1	1.4	0.2	0.1	0.1	0.9
	89.9	Evolve	47.3	0.7	14.9	8.4	14.0	11.7	1.5	0.2	0.1	0.1	0.9
CAMP	88.7	0.32	49.2	0.4	16.4	7.6	10.9	12.1	1.9	0.3	0.1	0.1	0.9
	89	0.32	49.1	0.4	16.3	7.7	11.2	12.0	1.9	0.3	0.1	0.1	0.9
	88.7	Evolve	49.2	0.4	16.5	7.6	10.6	12.2	1.9	0.3	0.1	0.1	0.9
	89	Evolve	49.1	0.4	16.3	7.7	11.2	12.0	1.9	0.3	0.1	0.1	0.9
MORB	89	0.32	48.9	0.9	17.1	7.2	10.5	11.8	2.4	0.0	0.1	0.1	0.9
	90.9	0.32	48.3	0.9	15.9	7.4	13.2	11.0	2.2	0.0	0.1	0.1	0.8
	89.9	0.32	48.6	0.9	16.6	7.3	11.8	11.4	2.3	0.0	0.1	0.1	0.8
	89	Evolve	48.9	0.9	17.2	7.2	10.3	11.9	2.4	0.0	0.1	0.1	0.9
	90.9	Evolve	48.2	0.8	15.8	7.4	13.6	10.9	2.2	0.0	0.1	0.1	0.8
	89.9	Evolve	48.6	0.9	16.6	7.3	11.8	11.4	2.3	0.0	0.1	0.1	0.8

equilibrium with the bulk magma to assess the possible temperature range due to Fo addition. We first adopt a universal terminal Fo content of 89, which serves as a minimum bound for our estimate of primary magma temperature. We also corrected to the highest Fo content observed in each magmatic suite if the highest-observed Fo was higher than 89. If the highest Fo represents the highest range of olivines precipitated, correcting to this value likely represents a maximum possible temperature. Finally, we also consider the mean Fo of all olivine crystals between Fo 89 and the observed maximum Fo for each province. The different temperatures estimated by these three different methods represent the minimum and maximum possible temperatures for each province. For the NAIP, we will use the observed range in temperatures coupled with a peridotite-melting model to examine if the high Fo olivines from the province can be petrogenetically related to the LIP.

When calculating the primary magma we used a fixed Fe/Mg exchange coefficient $K_D\,(Fe-Mg)^{Ol-liq}$ of 0.32, as well as the compositionally dependent Fe/Mg exchange coefficient $K_D\,(Fe-Mg)^{Ol-liq}$ of Tamura et al. [59]. An atomic Fe^{2+} to Fe^T ratio of 0.9 was assumed for an oxidation state [60]. More oxidized conditions will result in lower temperatures because the reduction in Fe^{2+} results in a higher Mg# of the primitive magma, requiring less olivine addition to reach equilibrium values. Temperatures and pressures were then calculated by simultaneously solving the silica barometer of Lee et al. [20] and the thermometer of Lee and Chin [61]. We then converted these apparent primary magma temperatures to effective mantle potential temperatures following the approach and equations from Katz et al. [62]. Primary magma compositions are reported in Table 1. Temperature and pressure results are reported in Table 2.

CAMP has no olivines with Fo higher than 89 so we used only our minimum of 89. By contrast, NAIP contains olivines with unusually high Fo (89-94.2). Correcting to these high values results in high temperatures. Using the selected primitive magmas determined in the previous section and back-adding olivine following the above scenarios give the following results. The minimum-observed mantle potential temperature is 1360°C for NAIP, 1320°C for CAMP, and 1310°C for MORB (Table 2). The maximum possible temperature (using highest-observed Fo) is 1620°C for NAIP, 1330°C for CAMP, and 1400°C for MORB (Table 2). Previous studies that concluded NAIP is hot used the unusually high Fo olivines observed as terminal olivines. Such high Fo olivines are not found in MORBs [10, 15, 24]. This difference in choice of terminal olivine results in >200°C difference in temperature estimates. Thus, the question is whether the high Fo olivines in NAIP or other provinces are appropriate terminal olivines. Below, we use the highest possible temperature for the NAIP, calculated using Fo 94.2, to constrain the highest possible peridotite melt fraction and therefore the highest Fo for the NAIP.

4.3. Are High Fo Contents in Olivine due to High Melt Fractions? In the previous section, we demonstrated the

Table 2: Temperatures of LIPs compared to MORB. Calculated olivine liquid and mantle potential temperatures using the primary magmas calculated in Table 1. The difference in temperatures reflects the variation in Fo and K_D $(Fe-Mg)^{Ol-liq}$. Temperatures and pressures were then calculated by simultaneously solving the silica barometer of Lee et al. [20] and the thermometer of Lee and Chin [61]. Mantle potential temperatures are calculated from the olivine-liquid temperatures and pressures using methods from Katz et al. [62]. The revised max Fo in the NAIP section refers to the maximum possible Fo content of the NAIP using melt fraction as a control. The revised mean Fo in the NAIP section refers to the mean Fo between the melt fraction constrained maximum Fo and the lower bound Fo of 89 set by average mantle olivine. Max observed in the CAMP section refers to the highest Fo olivine measured in the province. For comparison purposes, we back-add CAMP magmas to Fo 89 in the projected max section. DNE stands for Does Not Exist. To calculate mantle potential temperatures, the magma must intersect the solidus when back-correcting for the enthalpy of crystallization. Using a fixed K_D $(Fe-Mg)^{Ol-liq}$ and Fo of 94.2 gives such high temperatures and pressures that the magma will not intersect the solidus of Katz et al. [62] in the upper 10 GPa of the mantle, making calculating a potential temperature impossible. The fixed or evolving Kd refers to the K_D $(Fe-Mg)^{Ol-liq}$ used in Table 1 to calculate the primary magma by olivine addition.

Province	Forsterite content		T. olivine-liquid (C)		P (Gpa)		T.Ni mantle potential (C)	
NAIP	Min	89	1334	1337	1.2	1.2	1361	1363
	Max	94.2	1731	1828	5.7	8.0	DNE	1626
	Mean	91.04	1427	1452	1.9	2.1	1463	1488
	Revised max	90.94	1424	1436	1.9	2.0	1463	1466
	Revised mean	89.93	1387	1387	1.5	1.6	1419	1422
CAMP	Max observed	88.69	1295	1291	0.9	0.9	1316	1318
	Projected max	89	1307	1306	1.0	1.0	1335	1334
MORB	Min	89	1296	1293	1.0	1.0	1315	1312
	Max	90.85	1368	1374	1.5	1.5	1400	1403
	Mean	89.93	1328	1328	1.2	1.2	1351	1351
		Kd	Fixed	Evolving	Fixed	Evolving	Fixed	Evolving

sensitivity of temperature estimates to the assumed composition of the terminal olivine when correcting for fractional crystallization. High temperatures of NAIP in the literature are based on taking unusually high Fo olivines as the terminal olivine. Are these high Fo olivines appropriate to use as terminal olivine compositions for fractionation corrections? Here, we use the relationship between Fo and melt fraction (during melting of peridotite), the range of possible temperatures for the NAIP estimated above, and a peridotite-melting model to constrain the maximum Fo and therefore the temperature for the NAIP.

We use peridotite-melting models from Katz et al. [62] to explore plausible melt fractions that can be attained by decompression melting. Just prior to supercontinent break-up, any decompression melting is limited by the presence of a continental lithosphere, which reduces the headspace for decompression. We estimate plausible melt fractions under a lithospheric root for solid mantle potential temperatures ranging from 1300-1650°C (where mantle potential temperature refers to the temperature at Earth's surface if the solid mantle were adiabatically brought to the surface without melting). The maximum plausible mantle potential temperature for the NAIP, using an Fo of 94.2, is 1630°C for NAIP. In Katz et al.'s [62] model, melting commences at the depth and temperature corresponding to where the solid mantle adiabat, projected from the potential temperature at the Earth's surface, intersects the dry mantle solidus. From this intersection with the solidus, we allow the mantle to rise and adiabatically decompress and melt, continuing until it reaches the base of our model lithosphere. In our model, we use a dry fertile peridotite that contains 20% clinopyroxene. We ignore any possible compositional variations in the plume. We disregard pyroxenite melting because we are looking for the maximum possible melt fraction produced from peridotite, which will only decrease by the inclusion of pyroxenite [13, 24]. In a hypothetical model where the plume is composed only of harzburgite and peridotite, the calculated melt fraction of peridotite could increase [13, 24]. However, any increase will be small, because ultimately the exhaustion of clinopyroxene (shown in Figure 4 by the kink in the melting function) limits the possible melt contributions from a lherzolite source. Our single lithology model adequately captures the maximum limits on peridotite melting.

The continental lithosphere at the margins of the NAIP has undergone little extension; therefore, we can assume that the modern lithosphere-asthenosphere boundary beneath Greenland is a minimum bound on lithosphere thickness when the LIP erupted prior to continental break-up [63]. The depth of the lithosphere-asthenosphere boundary has been measured to be 120 km for Disco Island, 70 km for eastern Greenland, and 120-80 km for the Voring and Moring margins [64, 65]. We assume a lithospheric thickness of 90 km and an average lithosphere mantle density of 3300 kg/m^3, limiting decompression to minimum pressures of ~3 GPa. The maximum possible temperature estimated earlier for the NAIP was 1630°C. Lee and Chin's basalt thermometer has an error of less than 20°C [61]. Therefore, we

calculate the melting degree of the NAIP at 1650°C to get the upper bound of equilibrium Fo. For a lithospheric thickness of 90 km, a dry, fertile lherzolite with a mantle potential temperature of 1650°C can melt lherzolite only to 30% (Figure 4(b)). We use the observed relationship between Fo and melt fraction, assuming a y intercept of 89 and a slope of 15.70% melt fraction/Fo, to calculate that this melt fraction translates into an Fo content of 90.9 (Figure 4(a)). As an unrealistic upper bound, we can also assume that there is no lithosphere and allow the lherzolite mantle to reach the surface of the Earth, giving 45% melting degree as the highest attainable melt faction for a mantle potential temperature of 1650°C, corresponding to an Fo of 91.9. These results suggest that Fo values above 90.9 may require processes other than or in addition to primary mantle melting, and such olivine should not be used for estimating temperature. Such high Fo contents are more typical of Archean cratonic mantle or the mantle wedge beneath subduction zones [66–68]. Using the new maximum Fo value of 90.9, the highest possible mantle potential temperature for the NAIP is 1470°C (Tables 1 and 2).

For all scenarios, taking the highest-observed Fo olivine as the terminal olivine, even if they are not xenocrysts, may not be valid. Basalts represent the aggregate of polybaric melts formed by decompression melting [18]. The maximum Fo content in a polybaric-melting column corresponds to only the highest melt fractions in the column and is not representative of the integrated melt pathway [69]. It is the average Fo content or melting degree that is of interest, not the highest Fo content, which would reflect the very last stages of melting [19, 69]. For this reason, for a more realistic estimate of mantle temperatures we take the mean Fo of all olivines between Fo 89 and the observed or estimated (from the above estimates of melt fraction) maximum Fo. This mean is 89.93 for the NAIP and 90.85 for MORB. CAMP has no olivines above 89 so we use Fo 89. The resulting mantle potential temperature is 1420°C for the NAIP, 1330 for CAMP, and 1350 for MORB (Tables 1 and 2). With these maximum temperature estimates we do not observe a large enough temperature contrast between MORB, NAIP, and CAMP to support the LIP origin from a thermal plume.

4.4. The Formation of High Fo, High Ni Olivines in the NAIP. We now examine the origin of olivines with Fo higher than 90.9 in the NAIP. Above, we argued that these olivines require such high degrees of mantle melting that they could not have formed by decompression melting of a plume rising beneath continental lithosphere, due to the limited headspace for mantle upwelling. We thus concluded that the high Fo olivines are petrogenically unrelated to NAIP. Even so, it is still worth exploring the origin of these high Fo olivines. Olivine Fo >89 in basalts is unusual because basalts have usually differentiated to some extent by the time they reach the surface, leaving the most primitive olivines behind at depth. Olivine crystals in basalts with higher Fo either (1) reflect remarkable preservation of high-degree melting conditions, (2) represent xenocrysts from the lithospheric mantle, which itself may be the residue of high-degree mantle melting, or (3) represent olivines crystallized at the surface under highly oxidizing conditions, where Fe^{2+} is converted to Fe^{3+} and exsolved, leaving behind high Fo olivine [53, 70–72].

The high Fo olivines could have formed from the oxidation of the olivines during emplacement. In this scenario, the fayalite component in olivine is oxidized to Fe^{3+}, resulting in production of ferric-oxide phases and leaving behind a highly-forsteritic residual olivine [70]. Unusually, forsteritic olivines have been hypothesized to from in thick basaltic lava flows. An in-depth petrographic overview of high Fo olivines in the NAIP is beyond the scope of this study but would be valuable for further evaluating this hypothesis. We note, however, that such oxidation should not affect Ni as much as Fe and would thus predict high Fo olivines with low Ni contents, which is not what is seen (Figure 5).

We now explore the possibility that the high Fo olivines are xenocrysts. If true, the NAIP olivines should have the same melting and thermal histories—and therefore the same Ni and Fo contents—as olivines sourced from continental lithospheric mantle [52, 53]. We compared the Ni and Fo contents of the NAIP olivines to olivines from the Archean continental lithospheric mantle under Greenland, as well as olivines from the depleted mantle wedge of subduction zones [67, 73–75] (Figure 5). Our rationale for comparing to mantle wedge olivines was motivated by the possibility that subduction-related mantle may have been incorporated into the continental lithospheric mantle during continental collision. As can be seen from Figure 5, Greenland Archean cratonic olivines are too low in Ni to be the source for the NAIP olivines, but the harzburgite olivines from depleted mantle wedges have remarkably similar Ni and Fo contents to the high Fo, high Ni NAIP olivines.

4.5. On the Mantle Source Regions for the NAIP and CAMP. We now turn to characterizing the mantle sources of the NAIP and CAMP. As discussed earlier, Fe/Mn, Zn/Fe, and CaO/Al_2O_3 ratios are sensitive to the mineralogy of the melt source region. These ratios are minimally fractionated when melting peridotitic sources but are fractionated by melting of pyroxenites, yielding anomalous ratios [50]. As shown in Figure 3, the ratios of Fe/Mn, Zn/Fe, and CaO/Al_2O_3 for the NAIP and CAMP fall in the range expected of peridotite melting or are like MORB. Thus, these melts must be formed by peridotite melting or, if they are sourced from pyroxenites, the pyroxenites themselves must have originally derived by peridotite melting, and subsequent melting of pyroxenites occurred at high enough extents that the melt composition resembles the bulk composition of the system.

We have also used the Sm-Nd isotopic system to calculate a model age for separation from a depleted mantle source. NAIP and CAMP Nd isotopic compositions are less radiogenic than mid-ocean ridge basalts, which suggest derivation from an older, enriched source [44, 76]. We took the average whole-rock Nd isotopic composition from our NAIP and CAMP datasets and then calculated model ages using whole-rock Sm/Nd ratios. Depleted mantle and CHUR evolution lines were calculated using Sm/Nd data from Salters and Stracke [77] and Amelin and Rotenberg [78]. We estimate depleted mantle model ages of ~1.4 Ga for CAMP

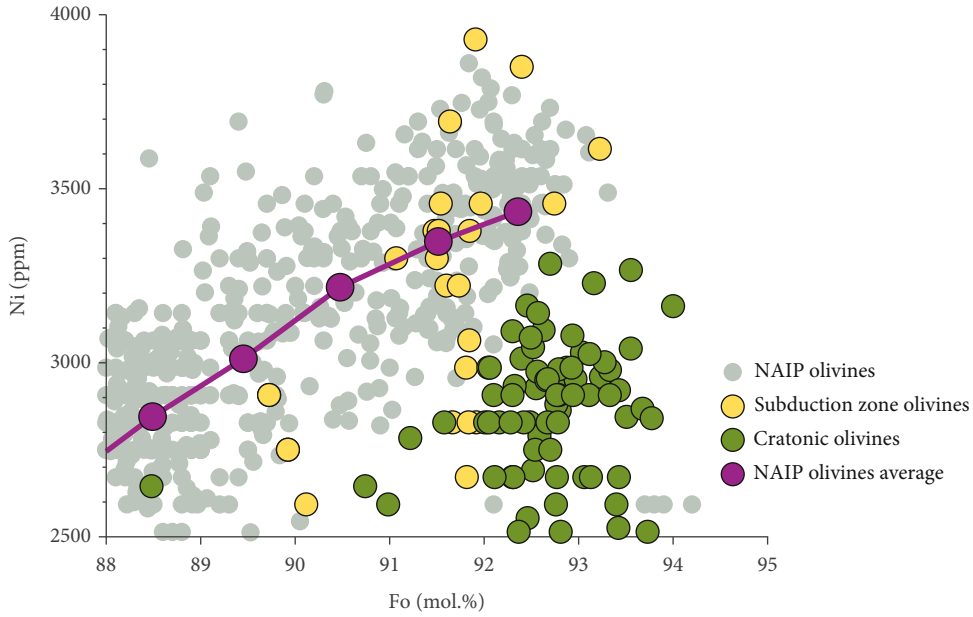

Figure 5: Binned NAIP olivine means are represented by purple circles. Individual samples are in light grey. Olivines from depleted harzburgite from former subduction zones are in yellow [67, 68]. Olivines from Greenland cratonic peridotite samples are in green [73–75]. Note that the depleted harzburgite olivines from subduction zones are similar in Fo and Ni to the high Ni, high Fo samples from the NAIP.

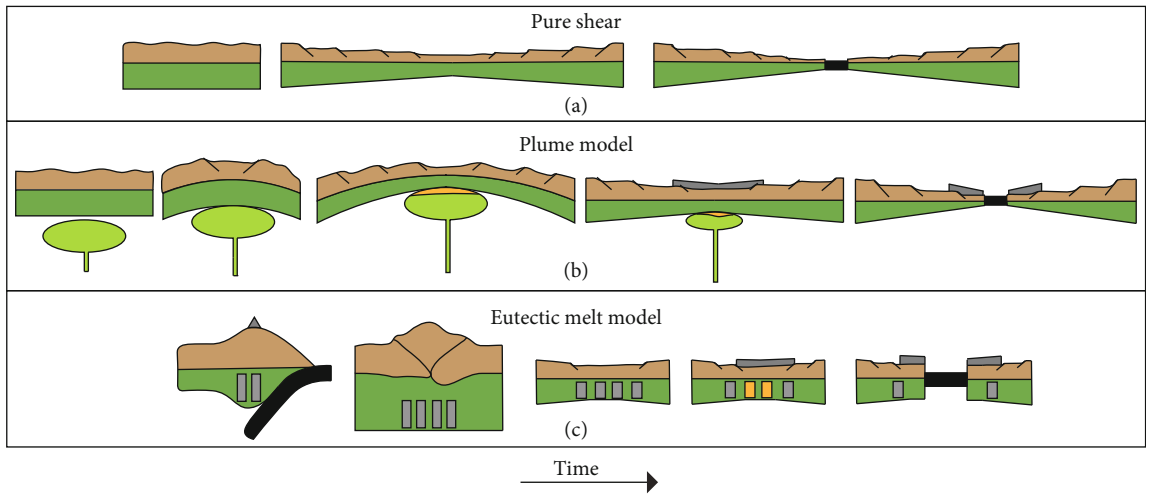

Figure 6: Different proposed models for continental rifting and LIP formation. (a) Continental break-up through pure shear with laterally homogeneous rheology. Without strain localization, this results in diffuse ocean-continent boundaries. Such a scenario does not produce significant amounts of magmas until rifting is complete. (b) In the plume model, hot and buoyant mantle upwells beneath a continent, resulting in uplift and gravitational collapse of the supercontinent. Impingement of plume head beneath the continent results in LIP formation. In such a scenario, LIPs would predate or be coeval with the initiation of rifting. (c) Eutectic melt model in which extension is driven by far-field stresses and LIP magmatism responds. Grey squares represent stalled arc pyroxenites. Orange squares represent melted pyroxenites. Fertile lithologies within the continental lithosphere melt when extension commences. These fertile lithologies may be inherited from prior events, such as subduction magmatism before supercontinent formation. If these fertile lithologies represent melts from the mantle, they would have eutectic-like compositions, which would then be characterized by high melt productivity such that once melting initiates, they would melt quickly without the need for extreme temperature anomalies. Such melting could also localize deformation, allowing for the generation of rapid ocean-continent transitions.

and ~0.7 Ga for NAIP. Although these model ages are highly uncertain, what is clear is that the sources for these LIPs are much older than their eruption ages. The NAIP and CAMP thus appear to derive from a peridotite source that is old.

4.6. Speculations on Rifting Models Compatible with a Low-Thermal Anomaly. Based on the above analysis, the NAIP and CAMP appear to come from a source with peridotitic elemental signatures at mantle potential temperatures like

that of MORBs. This raises a dilemma. A mantle source that is not anomalously hot along with the presence of a thick continental lithosphere would seem to preclude any high-degree melting, so how can the large amounts of magmas required to generate an LIP be generated under these conditions? High-degree melting, however, describes an intensive parameter and does not necessarily equate with absolute volume of magma generated. Here, we suggest how large volumes of low-degree melts could be responsible for generating some LIPs.

Insight into LIP genesis might come from geologic context. Both NAIP and CAMP are geographically close to ancient subduction zones. The western Greenland NAIP is located adjacent to the former Archean and Neoproterozoic arcs, while the eastern exposures of the NAIP are adjacent to Proterozoic and Ordovician arcs [79–84]. Similar relationships exist for CAMP, which formed in proximity to the remnants of old arcs during the Proterozoic, early Paleozoic (accretion of the Carolina terrain onto Laurentia), and late Paleozoic (Variscan arc on the Gondwana margin) [85–87]. It has also been recognized that some LIPs (CAMP and the Columbia River Flood Basalts) have subduction-like geochemical and isotopic signatures [26, 88, 89].

Motivated by the possible spatial association with ancient subduction zones, we speculate on a new model similar to that of Leeman and Harry [90]. First, during continental amalgamation, subduction zones actively produce magmatism through fractional melting as the previous ocean basin closes [86, 87, 91] (Figure 6(c), leftmost image). Some of this magma erupts to the surface, but a significant fraction fails to erupt, stalling out in the lithosphere as basaltic dikes [92–94]. If the stalled melts are primary melts and are produced by fractional melting, they will have eutectic compositions (Figure 7). Following Leeman and Harry [90], we propose a scenario in which these dike-forming magmas in the deep lithosphere represent trapped eutectic melts derived from the underlying asthenospheric mantle wedge.

The end of subduction culminates in ocean closure, continental collision, and the formation of a supercontinent [85, 87, 95] (Figure 6(c), second from the left image). We speculate that the dikes become entombed in the deep continental lithosphere of the orogeny, lying "dormant" until reactivated by subsequent continental break-up. Continental break-up ensues with initial extension related to orogenic collapse of a thickened orogen, followed by further extension controlled by far-field tectonic forces (Figure 6(c), middle image). As the continental lithosphere thins, the previously emplaced dikes decompress and melt (Figure 6(c), second from the right image). Because the dikes are near-eutectic melts of peridotite mantle, they mostly melt at the temperature of the eutectic, instead of over a large range of temperature [90] (Figures 7 and 6(c)). Due to the high melt productivity of eutectic lithologies, large amounts of melt could be generated in a short time without the need for anomalously high temperatures (Figure 7, path 3). In other words, large amounts of magmas with chemical signatures of a low-degree mantle melt (relative to peridotitic mantle) could be generated. While these dikes would likely be of pyroxenitic lithology [96]; at high melt fractions (relative to the dike),

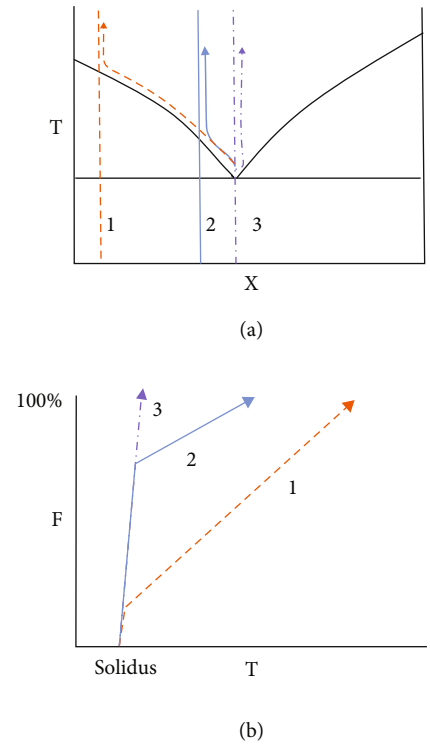

Figure 7: (a) Conceptual binary phase diagram showing a simple eutectic along with different bulk compositions 1, 2, and 3. Composition is on the x-axis and temperature on the y-axis. (b) Conceptual representation of melt productivity, where melt fraction (F) is plotted versus temperature. Curves labeled 1 through 3 correspond to melt productivity for the different bulk compositions noted in (a). In a simple binary with pure phases, melting begins at the eutectic temperature for all bulk compositions, and the system is not allowed to increase in temperature until one of the solid phases is consumed. In natural, multicomponent systems, melting is more complicated, but the overall behavior is still captured with this simple binary system. Importantly, if the bulk composition is of eutectic composition, melting occurs at the eutectic and over a small temperature range. Compositions that are far from the eutectic composition can only undergo high-degree melting if temperature increases well above the eutectic. Pyroxenite dikes in the lithospheric mantle formed as trapped melts would have near-eutectic bulk compositions and thus could undergo high degree remelting without significant increase in temperature.

the melt composition will resemble the bulk system (Figure 7, path 3), creating melts with Zn/Fe, Fe/Mn, and CaO/Al_2O_3 ratios that fall in the range of peridotite-derived melts (Figure 3).

Our speculative conceptual model makes testable predictions. First, because of the high melt productivity of dikes with eutectic-like compositions, not only are large amounts of magmas produced but these dikes would be quickly exhausted with further extension, resulting in a volumetrically large and temporally short pulse of magmatism. Once these lithospheric dikes are exhausted, further melting would have to occur by more conventional decompression melting of the asthenosphere, which would only occur after sufficient lithospheric extension [76]. Importantly, if the lithosphere is

transected by numerous ancient dikes, centered around ancient sutures, their melting would provide localized weak zones. It has been shown that in order to efficiently rift a continent to the point of generating thin oceanic crust, localized weak zones generated by the presence of melts are required [90, 97, 98]. However, such studies have not addressed the origin of localized melt zones. Our conceptual model provides a mechanism for generating these local rheological weak zones. Finally, the model explains the quick transition from thin oceanic to thick continental crust at continental margins, especially those associated with SDRs. The rheological weak zone provided by the dikes allows the continents to efficiently break, resulting in local rather than diffuse extension of the continental lithosphere and leading to rapid transition from continental to oceanic crust [63, 99] (Figure 6(c) compared to Figures 6(a) and 6(b)).

We fully admit that our model is highly speculative and is meant to drive debate in the scientific community. Our model does currently have flaws. One of the most notable problems is that our current model cannot neatly explain the trail of volcanism that follows the eruption of an LIP. It is possible that aseismic ridge observed at the NAIP and the enriched signal detected in MORB around Iceland is due to the entrainment of lithosphere pyroxenites into the upwelling mantle by edge-driven convection on the margins of cratonic lithospheric mantle root [76, 100, 101].

5. Conclusions

Mantle potential temperatures were calculated for the source regions of NAIP, CAMP, and MORB after evaluating the effects of olivine accumulation on the compositions of magmas. Our results show significant olivine accumulation in NAIP magmas and minor accumulation in CAMP and MORB magmas, resulting in reevaluation of true primitive magmas in the NAIP. The choice of terminal olivine composition used to correct for fractional crystallization was also reexamined, resulting in lower-forsterite values to be consistent with plausible melt fractions. Based on these considerations, we estimated potential temperatures of 1420°C for the NAIP, 1330°C for CAMP, and 1350°C for MORB. The small temperature contrast between these two LIPs and MORBs suggests that the NAIP and CAMP were not associated with deep-seated thermal plumes, which would be >200°C than ambient mantle. Elemental and radiogenic isotope systematics suggest that these LIP source regions have a peridotitic signature but are older than the LIPs themselves. Our results raise a dilemma. Generating large amounts of melt from a peridotitic mantle beneath thick lithosphere is not possible without a thermal anomaly. However, fertile lithologies embedded within the continental lithosphere could undergo preferential melting during the initial stages of supercontinent break-up. If these lithologies were eutectic-like melts trapped within the lithosphere during the processes leading up to supercontinent assembly, they would be characterized by high melt productivity and peridotitic trace element signatures. Melting of these lithologies, triggered by extension, would not only generate LIPs but generate weak zones necessary to give the localized deformation needed for continental break-up.

Data Availability

Data were downloaded from the EarthChem online database and then further supplemented with a literature review (http://earthchem.org/portal). The compiled data and complete reference list are included in supplementary file 1.

Disclosure

This manuscript was significantly improved by the reviews of Steve Barnes, Lorenzo Fedele, and two anonymous reviewers.

Conflicts of Interest

The authors declare that they have no conflicts of interest.

Acknowledgments

This work was supported by a grant from the United States National Science Foundation (NSF EAR-2139558) to Lee and the Geological Society of America Grants-in-Aid of research and the Alaskan Geological Society to Borchardt. We thank Jolante Van Der Wijk, Dennis Harry, and Micah Mayle for their discussions and insight.

Supplementary Materials

Supplementary File 1: whole-rock and olivine chemical data used in this study along with a complete reference list. *(Supplementary Materials)*

References

[1] R. Damian Nance and J. Brendan Murphy, "Origins of the supercontinent cycle," *Geoscience Frontiers*, vol. 4, no. 4, pp. 439–448, 2013.

[2] G. M. Young, "Precambrian supercontinents, glaciations, atmospheric oxygenation, metazoan evolution and an impact that may have changed the second half of Earth history," *Geoscience Frontiers*, vol. 4, no. 3, pp. 247–261, 2013.

[3] N. Eyles, "Glacio-epochs and the supercontinent cycle after ~ 3.0 Ga: tectonic boundary conditions for glaciation," *Palaeogeography Palaeoclimatology Palaeoecology*, vol. 258, no. 1-2, pp. 89–129, 2008.

[4] P. F. Hoffman, A. J. Kaufman, G. P. Halverson, and D. P. Schrag, "A Neoproterozoic snowball earth," *Science*, vol. 281, no. 5381, pp. 1342–1346, 1998.

[5] I. H. Campbell and C. M. Allen, "Formation of supercontinents linked to increases in atmospheric oxygen," *Nature Geoscience*, vol. 1, no. 8, pp. 554–558, 2008.

[6] N. R. Meyer, A. E. Parada, B. J. Kapili, J. L. Fortney, and A. E. Dekas, "Rates and physicochemical drivers of microbial anabolic activity in deep-sea sediments and implications for deep time," *Environmental Microbiology*, vol. 24, no. 11, 2022.

[7] P. F. Hoffman, "The break-up of Rodinia, birth of Gondwana, true polar wander and the snowball Earth," *Journal of African Earth Sciences*, vol. 28, no. 1, pp. 17–33, 1999.

[8] I. W. D. Dalziel, L. A. Lawver, and J. B. Murphy, "Plumes, orogenesis, and supercontinental fragmentation," *Earth and Planetary Science Letters*, vol. 178, no. 1-2, pp. 1–11, 2000.

[9] G. R. Foulger, "Plumes, or plate tectonic processes?," *Astronomy and Geophysics*, vol. 43, no. 6, pp. 6.19–6.23, 2002.

[10] K. D. Putirka, "Mantle potential temperatures at Hawaii, Iceland, and the mid-ocean ridge system, as inferred from olivine phenocrysts: evidence for thermally driven mantle plumes," *Geochemistry, Geophysics, Geosystems*, vol. 6, no. 5, 2005.

[11] N. H. Sleep, "Mantle plumes?," *Astronomy and Geophysics*, vol. 44, no. 1, pp. 1.11–1.13, 2003.

[12] B. C. Storey, "The role of mantle plumes in continental breakup: case histories from Gondwanaland," *Nature*, vol. 377, 1995.

[13] O. Shorttle, J. Maclennan, and S. Lambart, "Quantifying lithological variability in the mantle," *Earth and Planetary Science Letters*, vol. 395, pp. 24–40, 2014.

[14] R. White and D. McKenzie, "Magmatism at rift zones: the generation of volcanic continental margins and flood basalts," *Journal of Geophysical Research - Solid Earth*, vol. 94, no. B6, pp. 7685–7729, 1989.

[15] C. Herzberg and E. Gazel, "Petrological evidence for secular cooling in mantle plumes," *Nature*, vol. 458, no. 458, p. 7238, 2009.

[16] K. D. Putirka, M. Perfit, F. J. Ryerson, and M. G. Jackson, "Ambient and excess mantle temperatures, olivine thermometry, and active vs. passive upwelling," *Chemical Geology*, vol. 241, no. 3-4, pp. 177–206, 2007.

[17] K. Putirka, Y. Tao, K. R. Hari, M. R. Perfit, M. G. Jackson, and R. Arevalo, "The mantle source of thermal plumes: trace and minor elements in olivine and major oxides of primitive liquids (and why the olivine compositions don't matter)," *American Mineralogist*, vol. 103, no. 8, pp. 1253–1270, 2018.

[18] P. L. Roeder and R. F. Emslie, "Olivine-liquid equilibrium," *Contributions to Mineralogy and Petrology*, vol. 29, no. 4, pp. 275–289, 1970.

[19] C. Herzberg, P. D. Asimow, N. Arndt et al., "Temperatures in ambient mantle and plumes: constraints from basalts, picrites, and komatiites," *Geochemistry, Geophysics, Geosystems*, vol. 8, no. 2, 2007.

[20] C.-T. A. Lee, P. Luffi, T. Plank, H. Dalton, and W. P. Leeman, "Constraints on the depths and temperatures of basaltic magma generation on Earth and other terrestrial planets using new thermobarometers for mafic magmas," *Earth and Planetary Science Letters*, vol. 279, no. 1-2, pp. 20–33, 2009.

[21] C. Herzberg and M. J. O'hara, "Plume-associated ultramafic magmas of Phanerozoic age," *Journal of Petrology*, vol. 43, no. 10, pp. 1857–1883, 2002.

[22] L. A. Coogan, A. D. Saunders, and R. N. Wilson, "Aluminum-in-olivine thermometry of primitive basalts: evidence of an anomalously hot mantle source for large igneous provinces," *Chemical Geology*, vol. 368, pp. 1–10, 2014.

[23] Z. Wan, L. A. Coogan, and D. Canil, "Experimental calibration of aluminum partitioning between olivine and spinel as a geothermometer," *American Mineralogist*, vol. 93, no. 7, pp. 1142–1147, 2008.

[24] S. Matthews, K. Wong, O. Shorttle, M. Edmonds, and J. Maclennan, "Do olivine crystallization temperatures faithfully record mantle temperature variability?," *Geochemistry, Geophysics, Geosystems*, vol. 22, no. 4, article e2020GC009157, 2021.

[25] H. E. Spice, J. G. Fitton, and L. A. Kirstein, "Temperature fluctuation of the Iceland mantle plume through time," *Geochemistry, Geophysics, Geosystems*, vol. 17, no. 2, pp. 243–254, 2016.

[26] L. Whalen, E. Gazel, C. Vidito et al., "Supercontinental inheritance and its influence on supercontinental breakup: the Central Atlantic magmatic province and the breakup of Pangea," *Geochemistry, Geophysics, Geosystems*, vol. 16, no. 10, pp. 3532–3554, 2015.

[27] M. R. Perfit, D. J. Fornari, W. I. Ridley et al., "Recent volcanism in the Siqueiros transform fault: picritic basalts and implications for MORB magma genesis," *Earth and Planetary Science Letters*, vol. 141, no. 1-4, pp. 91–108, 1996.

[28] J. Á. Horni, J. R. Hopper, A. Blischke et al., "Regional distribution of volcanism within the North Atlantic Igneous Province," *Geological Society of London, Special Publication*, vol. 447, no. 1, pp. 105–125, 2017.

[29] C. M. Wilkinson, M. Ganerød, B. W. H. Hendriks, and E. A. Eide, "Compilation and appraisal of geochronological data from the North Atlantic Igneous Province (NAIP)," *Geological Society of London, Special Publication*, vol. 447, no. 1, pp. 69–103, 2017.

[30] T. B. Andersen, "Extensional tectonics in the Caledonides of Southern Norway, an overview," *Tectonophysics*, vol. 285, no. 3-4, pp. 333–351, 1998.

[31] A. G. Doré, E. R. Lundin, L. N. Jensen, Ø. Birkeland, P. E. Eliassen, and C. Fichler, "Principal tectonic events in the evolution of the northwest European Atlantic margin," *Geological Society, London, Petroleum Geology Conference Series*, vol. 5, no. 1, pp. 41–61, 1999.

[32] C. Gaina, A. Nasuti, G. S. Kimbell, and A. Blischke, "Break-up and seafloor spreading domains in the NE Atlantic," *Geological Society of London, Special Publication*, vol. 447, no. 1, pp. 393–417, 2017.

[33] T. J. Blackburn, P. E. Olsen, S. A. Bowring et al., "Zircon U-Pb geochronology links the end-Triassic extinction with the Central Atlantic magmatic province," *Science*, vol. 340, no. 6135, pp. 941–945, 2013.

[34] A. Marzoli, S. Callegaro, J. Dal Corso et al., "The Central Atlantic magmatic province (CAMP): a review," in *The Late Triassic World: Earth in a Time of Transition*, L. H. Tanner, Ed., pp. 91–125, Springer International Publishing, Cham, 2018.

[35] P. Olsen, "Stratigraphic record of the early Mesozoic breakup of Pangea in the Laurasia-Gondwana rift system," *Annual Review of Earth and Planetary Sciences*, vol. 25, pp. 337–401, 2003.

[36] R. I. Hill, "Starting plumes and continental break-up," *Earth and Planetary Science Letters*, vol. 104, no. 2-4, pp. 398–416, 1991.

[37] J. A. Barrat and R. W. Nesbitt, "Geochemistry of the Tertiary volcanism of Northern Ireland," *Chemical Geology*, vol. 129, no. 1-2, pp. 15–38, 1996.

[38] H. Hansen, A. K. Pedersen, R. A. Duncan et al., "Volcanic stratigraphy of the southern Prinsen af Wales Bjerge region, East Greenland," *Geological Society of London, Special Publication*, vol. 197, no. 1, pp. 183–218, 2002.

[39] A. C. Kerr, R. W. Kent, B. A. Thomson, J. K. Seedhouse, and C. H. Donaldson, "Geochemical evolution of the tertiary Mull volcano, Western Scotland," *Journal of Petrology*, vol. 40, no. 6, pp. 873–908, 1999.

[40] L. M. Larsen and A. K. Pedersen, "Petrology of the Paleocene picrites and flood basalts on Disko and Nuussuaq, West Greenland," *Journal of Petrology*, vol. 50, no. 9, pp. 1667–1711, 2009.

[41] N. Søager and P. M. Holm, "Changing compositions in the Iceland plume; isotopic and elemental constraints from the Paleogene Faroe flood basalts," *Chemical Geology*, vol. 280, no. 3-4, pp. 297–313, 2011.

[42] N. A. Starkey, F. M. Stuart, R. M. Ellam, J. G. Fitton, S. Basu, and L. M. Larsen, "Helium isotopes in early Iceland plume picrites: constraints on the composition of high $^{3}He/^{4}He$ mantle," *Earth and Planetary Science Letters*, vol. 277, no. 1–2, pp. 91–100, 2009.

[43] H. Bertrand, J. Dostal, and C. Dupuy, "Geochemistry of early mesozoic tholeiites from Morocco," *Earth and Planetary Science Letters*, vol. 58, no. 2, pp. 225–239, 1982.

[44] S. Callegaro, C. Rapaille, A. Marzoli et al., "Enriched mantle source for the Central Atlantic magmatic province: new supporting evidence from southwestern Europe," *Lithos*, vol. 188, pp. 15–32, 2014.

[45] R. V. Fodor, A. N. Sial, S. B. Mukasa, and E. H. McKee, "Petrology, isotope characteristics, and K-Ar ages of the Maranhão, northern Brazil, Mesozoic basalt province," *Contributions to Mineralogy and Petrology*, vol. 104, no. 5, pp. 555–567, 1990.

[46] D. Gottfried, A. J. Froelich, and J. N. Grossman, "Geochemical data for Jurassic diabase associated with early Mesozoic basins in the eastern United States; Danville basin and vicinity, Virginia," *Open-File Report*, vol. 91-322-H, 1991.

[47] R. Batiza and Y. Niu, "Petrology and magma chamber processes at the East Pacific rise ~ 9°30′N," *Journal of Geophysical Research*, vol. 97, no. B5, pp. 6779–6797, 1992.

[48] G. Thompson, W. Bryan, and S. Humphris, "Axial volcanism on the East Pacific rise, 10–12°N," *Geological Society of London, Special Publication*, vol. 42, no. 1, pp. 181–200, 1989.

[49] V. D. Wanless, M. R. Perfit, E. M. Klein, S. White, and W. I. Ridley, "Reconciling geochemical and geophysical observations of magma supply and melt distribution at the 9°N overlapping spreading center, East Pacific Rise," *Geochemistry, Geophysics, Geosystems*, vol. 13, no. 11, 2012.

[50] V. Le Roux, C.-T. A. Lee, and S. J. Turner, "Zn/Fe systematics in mafic and ultramafic systems: implications for detecting major element heterogeneities in the Earth's mantle," *Geochimica et Cosmochimica Acta*, vol. 74, no. 9, pp. 2779–2796, 2010.

[51] L. Qin and M. Humayun, "The Fe/Mn ratio in MORB and OIB determined by ICP-MS," *Geochimica et Cosmochimica Acta*, vol. 72, no. 6, pp. 1660–1677, 2008.

[52] A. K. Matzen, M. B. Baker, J. R. Beckett, and E. M. Stolper, "The temperature and pressure dependence of nickel partitioning between olivine and silicate melt," *Journal of Petrology*, vol. 54, no. 12, pp. 2521–2545, 2013.

[53] A. K. Matzen, M. B. Baker, J. R. Beckett, B. J. Wood, and E. M. Stolper, "The effect of liquid composition on the partitioning of Ni between olivine and silicate melt," *Contributions to Mineralogy and Petrology*, vol. 172, no. 1, p. 3, 2017.

[54] K. Chau, *Mineral chemistry and origin of the olivine-rich zone of the palisades sill, [M.S. thesis]*, Florida International University, 2009.

[55] J. N. Grossman, D. Gottfried, and A. J. Froelich, "Geochemical data for Jurassic diabase associated with early Mesozoic basins in the eastern United States," *Open-File Report*, vol. 91-322, 1991.

[56] R. Dasgupta, M. G. Jackson, and C.-T. A. Lee, "Major element chemistry of ocean island basalts – conditions of mantle melting and heterogeneity of mantle source," *Earth and Planetary Science Letters*, vol. 289, no. 3-4, pp. 377–392, 2010.

[57] R. Xu, Y. Liu, and S. Lambart, "Melting of a hydrous peridotite mantle source under the Emeishan large igneous province," *Earth Science Reviews*, vol. 207, article 103253, 2020.

[58] M. J. Walter, "Melting of garnet peridotite and the origin of komatiite and depleted lithosphere," *Journal of Petrology*, vol. 39, no. 1, pp. 29–60, 1998.

[59] Y. Tamura, M. Yuhara, and T. Ishii, "Primary arc basalts from Daisen volcano, Japan: equilibrium crystal fractionation versus disequilibrium fractionation during supercooling," *Journal of Petrology*, vol. 41, no. 3, pp. 431–448, 2000.

[60] A. Bézos and E. Humler, "The $Fe^{3+}/\Sigma Fe$ ratios of MORB glasses and their implications for mantle melting," *Geochimica et Cosmochimica Acta*, vol. 69, no. 3, pp. 711–725, 2005.

[61] C.-T. A. Lee and E. J. Chin, "Calculating melting temperatures and pressures of peridotite protoliths: implications for the origin of cratonic mantle," *Earth and Planetary Science Letters*, vol. 403, pp. 273–286, 2014.

[62] R. F. Katz, M. Spiegelman, and C. H. Langmuir, "A new parameterization of hydrous mantle melting," *Geochemistry, Geophysics, Geosystems*, vol. 4, no. 9, 2003.

[63] E. R. Lundin, A. G. Doré, J. Naliboff, and J. V. Wijk, "Utilization of continental transforms in break-up: observations, models, and a potential link to magmatism," *Geological Society of London, Special Publication*, vol. 524, no. 1, 2022.

[64] M. Fernàndez, C. Ayala, M. Torne, J. Vergés, M. Gómez, and R. Karpuz, "Lithospheric structure of the mid-Norwegian margin: comparison between the Møre and Vøring margins," *Journal of the Geological Society*, vol. 162, no. 6, pp. 1005–1012, 2005.

[65] P. Kumar, R. Kind, W. Hanka et al., "The lithosphere-asthenosphere boundary in the North-West Atlantic region," *Earth and Planetary Science Letters*, vol. 236, no. 1-2, pp. 249–257, 2005.

[66] C.-T. A. Lee, P. Luffi, and E. J. Chin, "Building and destroying continental mantle," *Annual Review of Earth and Planetary Sciences*, vol. 39, no. 1, pp. 59–90, 2011.

[67] S. Song, L. Su, Y. Niu, Y. Lai, and L. Zhang, "CH_4 inclusions in orogenic harzburgite: evidence for reduced slab fluids and implication for redox melting in mantle wedge," *Geochimica et Cosmochimica Acta*, vol. 73, no. 6, pp. 1737–1754, 2009.

[68] H. Sumino, R. Burgess, T. Mizukami, S. R. Wallis, G. Holland, and C. J. Ballentine, "Seawater-derived noble gases and halogens preserved in exhumed mantle wedge peridotite," *Earth and Planetary Science Letters*, vol. 294, no. 1-2, pp. 163–172, 2010.

[69] P. D. Asimow, M. M. Hirschmann, and E. M. Stolper, "Calculation of peridotite partial melting from thermodynamic models of minerals and melts, IV. Adiabatic decompression and the composition and mean properties of mid-ocean ridge basalts," *Journal of Petrology*, vol. 42, no. 5, pp. 963–998, 2001.

[70] M. S. Blondes, M. T. Brandon, P. W. Reiners, F. Z. Page, and N. T. Kita, "Generation of forsteritic olivine (Fo99·8) by subsolidus oxidation in basaltic flows," *Journal of Petrology*, vol. 53, no. 5, pp. 971–984, 2012.

[71] J. Korenaga and P. B. Kelemen, "Major element heterogeneity in the mantle source of the North Atlantic igneous province," *Earth and Planetary Science Letters*, vol. 184, no. 1, pp. 251–268, 2000.

[72] A. V. Sobolev, A. W. Hofmann, S. V. Sobolev, and I. K. Nikogosian, "An olivine-free mantle source of Hawaiian shield basalts," *Nature*, vol. 434, no. 7033, pp. 590–597, 2005.

[73] S. Bernstein, P. B. Kelemen, and C. K. Brooks, "Depleted spinel harzburgite xenoliths in Tertiary dykes from East Greenland: restites from high degree melting," *Earth and Planetary Science Letters*, vol. 154, no. 1-4, pp. 221–235, 1998.

[74] S. Bernstein, K. Hanghøj, P. B. Kelemen, and C. K. Brooks, "Ultra-depleted, shallow cratonic mantle beneath West Greenland: dunitic xenoliths from Ubekendt Ejland," *Contributions to Mineralogy and Petrology*, vol. 152, no. 3, pp. 335–347, 2006.

[75] S. Bernstein, P. B. Kelemen, and K. Hanghøj, "Consistent olivine mg# in cratonic mantle reflects Archean mantle melting to the exhaustion of orthopyroxene," *Geology*, vol. 35, no. 5, pp. 459–462, 2007.

[76] A. Agranier, R. C. Maury, L. Geoffroy, F. Chauvet, B. Le Gall, and A. R. Viana, "Volcanic record of continental thinning in Baffin Bay margins: insights from Svartenhuk Halvø Peninsula basalts, West Greenland," *Lithos*, vol. 334-335, pp. 117–140, 2019.

[77] V. J. M. Salters and A. Stracke, "Composition of the depleted mantle," *Geochemistry, Geophysics, Geosystems*, vol. 5, no. 5, 2004.

[78] Y. Amelin and E. Rotenberg, "Sm-Nd systematics of chondrites," *Earth and Planetary Science Letters*, vol. 223, no. 3-4, pp. 267–282, 2004.

[79] E. Badenszki, J. S. Daly, M. J. Whitehouse, A. Kronz, B. G. J. Upton, and M. S. A. Horstwood, "Age and origin of deep crustal meta-igneous xenoliths from the Scottish Midland Valley: vestiges of an early Palaeozoic arc and 'newer granite' magmatism," *Journal of Petrology*, vol. 60, no. 8, pp. 1543–1574, 2019.

[80] J. N. Connelly and B. Ryan, "Late Archean evolution of the Nain Province, Nain, Labrador: imprint of a collision," *Canadian Journal of Earth Sciences*, vol. 33, no. 9, pp. 1325–1342, 1996.

[81] F. Kalsbeek and A. P. Nutman, "Anatomy of the early Proterozoic Nagssugtoqidian orogen, West Greenland, explored by reconnaissance SHRIMP U-Pb zircon dating," *Geology*, vol. 24, no. 6, pp. 515–518, 1996.

[82] G. B. Meyer, T. Grenne, and R. B. Pedersen, "Age and tectonic setting of the Nesåa Batholith: implications for Ordovician arc development in the Caledonides of Central Norway," *Geological Magazine*, vol. 140, no. 5, pp. 573–594, 2003.

[83] A. Nutman, F. Kalsbeek, and C. Friend, "The Nagssugtoqidian Orogen in south-east Greenland: evidence for Paleoproterozoic collision and plate assembly," *American Journal of Science*, vol. 308, no. 4, pp. 529–572, 2008.

[84] B. F. Windley and A. A. Garde, "Arc-generated blocks with crustal sections in the North Atlantic craton of West Greenland: crustal growth in the Archean with modern analogues," *Earth Science Reviews*, vol. 93, no. 1-2, pp. 1–30, 2009.

[85] M. Domeier and T. H. Torsvik, "Plate tectonics in the late Paleozoic," *Geoscience Frontiers*, vol. 5, no. 3, pp. 303–350, 2014.

[86] J. P. Hibbard, E. F. Stoddard, D. T. Secor, and A. J. Dennis, "The Carolina Zone: overview of Neoproterozoic to early Paleozoic peri- Gondwanan terranes along the eastern flank of the southern Appalachians," *Earth Science Reviews*, vol. 57, no. 3-4, pp. 299–339, 2002.

[87] A. Michard, A. Soulaimani, C. Hoepffner et al., "The southwestern branch of the Variscan belt: evidence from Morocco," *Tectonophysics*, vol. 492, no. 1-4, pp. 1–24, 2010.

[88] E. B. Cahoon, M. J. Streck, A. A. P. Koppers, and D. P. Miggins, "Reshuffling the Columbia River Basalt chronology—-Picture Gorge Basalt, the earliest- and longest-erupting formation," *Geology*, vol. 48, no. 4, pp. 348–352, 2020.

[89] J. H. Puffer, "Contrasting high field strength element contents of continental flood basalts from plume versus reactivated-arc sources," *Geology*, vol. 29, no. 8, pp. 675–678, 2001.

[90] W. P. Leeman and D. L. Harry, "A binary source model for extension-related magmatism in the Great Basin, Western North America," *Science*, vol. 262, no. 5139, pp. 1550–1554, 1993.

[91] C. R. van Staal, J. B. Whalen, V. J. McNicoll et al., "The Notre Dame arc and the Taconic orogeny in Newfoundland," *Memoir - Geological Society of America*, vol. 200, pp. 511–552, 2007.

[92] C. Annen and R. S. J. Sparks, "Effects of repetitive emplacement of basaltic intrusions on thermal evolution and melt generation in the crust," *Earth and Planetary Science Letters*, vol. 203, no. 3-4, pp. 937–955, 2002.

[93] G. W. Bergantz, "Underplating and partial melting: implications for melt generation and extraction," *Science*, vol. 245, no. 4922, pp. 1093–1095, 1989.

[94] F. Raia and F. J. Spera, "Simulations of crustal anatexis: implications for the growth and differentiation of continental crust," *Journal of Geophysical Research - Solid Earth*, vol. 102, no. B10, pp. 22629–22648, 1997.

[95] C. R. V. Staal, J. F. Dewey, C. M. Niocaill, and W. S. McKerrow, "The Cambrian-Silurian tectonic evolution of the northern Appalachians and British Caledonides: history of a complex, West and Southwest Pacific-type segment of Iapetus," *Geological Society of London, Special Publication*, vol. 143, no. 1, pp. 197–242, 1998.

[96] T. Kogiso, M. M. Hirschmann, and M. Pertermann, "High-pressure partial melting of mafic lithologies in the mantle," *Journal of Petrology*, vol. 45, no. 12, pp. 2407–2422, 2004.

[97] R. W. Bialas, W. R. Buck, and R. Qin, "How much magma is required to rift a continent?," *Earth and Planetary Science Letters*, vol. 292, no. 1-2, pp. 68–78, 2010.

[98] W. R. Buck, "1. Consequences of asthenospheric variability on continental rifting," in *Rheology and Deformation of the Lithosphere at Continental Margins*, pp. 1–30, Columbia University Press, 2004.

[99] M. O. Withjack, R. W. Schlische, and P. E. Olsen, "Development of the passive margin of eastern North America," in *Regional Geology and Tectonics: Phanerozoic Rift Systems and Sedimentary Basins*, pp. 300–335, Elsevier, 2012.

[100] S. F. Foley, "Rejuvenation and erosion of the cratonic lithosphere," *Nature Geoscience*, vol. 1, no. 8, pp. 503–510, 2008.

[101] B. J. Murton, R. N. Taylor, and M. F. Thirlwall, "Plume-ridge interaction: a geochemical perspective from the Reykjanes Ridge," *Journal of Petrology*, vol. 43, no. 11, pp. 1987–2012, 2002.